Supporting Information

Chemically Stable Ionic Viologen-Organic Network: An Efficient Scavenger of Toxic Oxo-anions from Water

Partha Samanta,[a] Priyanshu Chandra,[†,a] Subhajit Dutta,[†,a] Aamod V. Desai[a] and Sujit K. Ghosh*[a,b]

[a] Department of Chemistry, Indian Institute of Science Education and Research, Dr. Homi Bhabha Road, Pashan, Pune 411008, India. Phone: +91 20 2590 8076; E-mail: sghosh@iiserpune.ac.in

[b] Centre for Energy Science, IISER Pune, Dr. Homi Bhabha Road, Pashan, Pune 411008, India.

[†] These authors contributed equally.

Experimental Section:

FE-SEM analysis:

For solid-state analysis <1 mg sample was adhered on double sided carbon tape and hence used for FE-SEM imaging. FESEM was done by using FEI Quanta 3D dual beam ESEM at 30 KV.

Adsorption isotherm experiment:

Compound-1 (5 mg) was immersed in 2 mL water solution of oxo-anion having different concentration (in case of CrO_4^{2-} ion concentration was taken in the range of 29-580 ppm and for ReO_4^- ion the range of concentration is 62.5-1251 ppm). After 2 hours UV-Visible spectroscopy was carried out with the supernatant solution and further fitted with following equation,

Langmuir model, $$Q_e = \frac{Q_m C_e}{K_d + C_e}$$

where, C_e (ppm) and Q_e (mg gm^{-1}) are the oxo-anion concentration at equilibrium and amount of oxo-anion adsorbed at equilibrium respectively. Q_m (mg gm^{-1}) is the maximum amount of oxo-anion per unit mass of adsorbent to form a complete monolayer. K_d (mg/L) is a constant related to the affinity of the binding sites.

Freundlich Model, $$Q_e = K_F C_e^{1/n}$$

where, K_F and 1/n are the Freundlich model constants, indicating capacity and intensity of adsorption, respectively.

pH-dependent capture study:

Compound-1 (2 mg) was immersed in 2 mL solution of 2.5 mM oxo-anion (in case of CrO_4^{2-} ion pH-1.7, pH-4, pH-9, pH-10 and pH-12.4 were used, whereas for ReO_4^- ion pH-9, pH-10 and pH-12.4 were used) and stirred for 24 hours. After 1 day UV-Vis study was carried out to check the removal efficiency of compound-1. Following equation has been used for calculation and compared with the data at pH-7 for relative performance,

$$D_t = \frac{C_0 - C_t}{C_0} \times 100\% = \frac{A_0 - A_t}{A_0} \times 100\%$$

Where, D_t is the exchange capacity, C_0 and A_0 are initial concentration and absorbance of the oxo-anion solution respectively, C_t and A_t, are concentration and absorbance of the oxo-anion solution at specific times respectively.

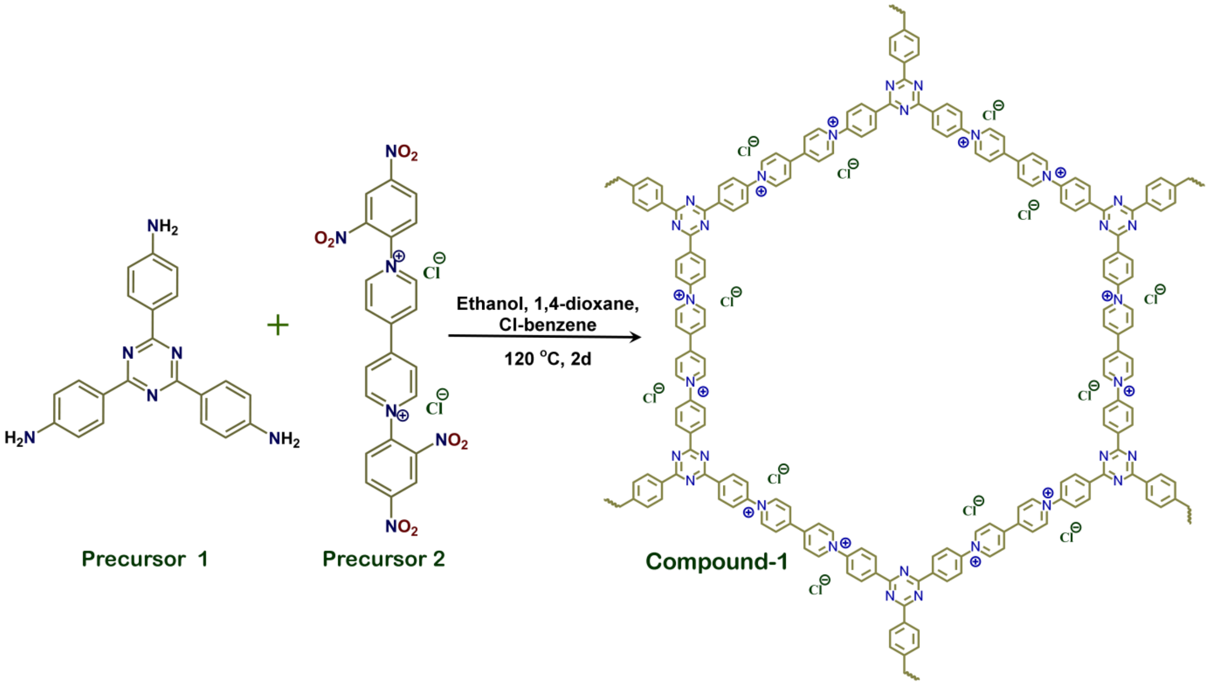

Scheme S1: Synthesis scheme of compound-1.

Figures:

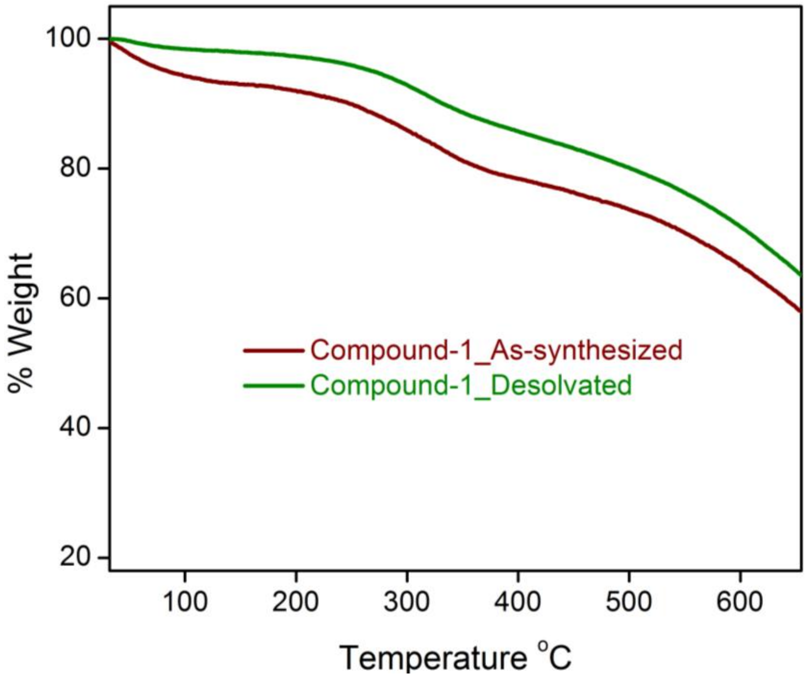

Figure S1: Thermogravimetric analysis (TGA) of as-synthesized compound-1 (wine red) and desolvated phase of compound-1 (green).

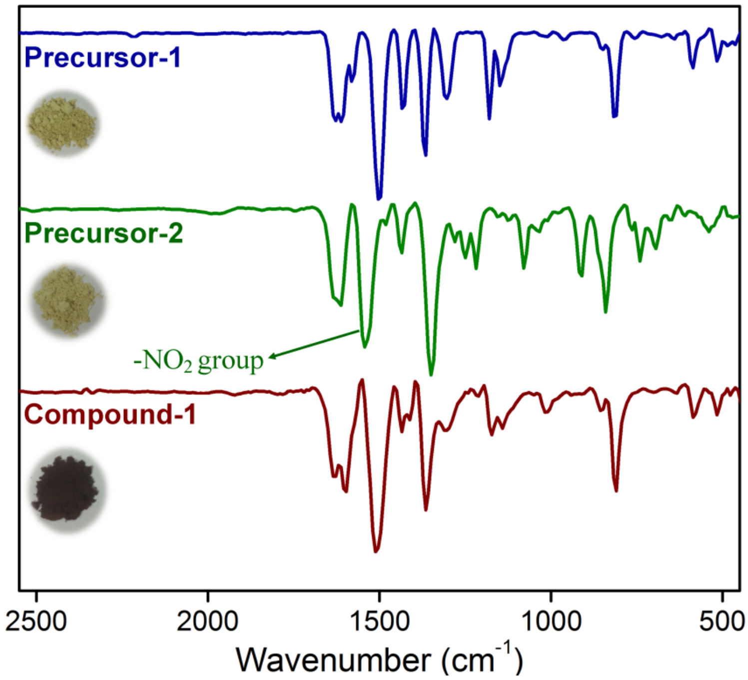

Figure S2: Infra-red (IR) spectroscopy of starting materials [precursor 1 (blue) and precursor 2 (green)] and compound-1 (wine red).

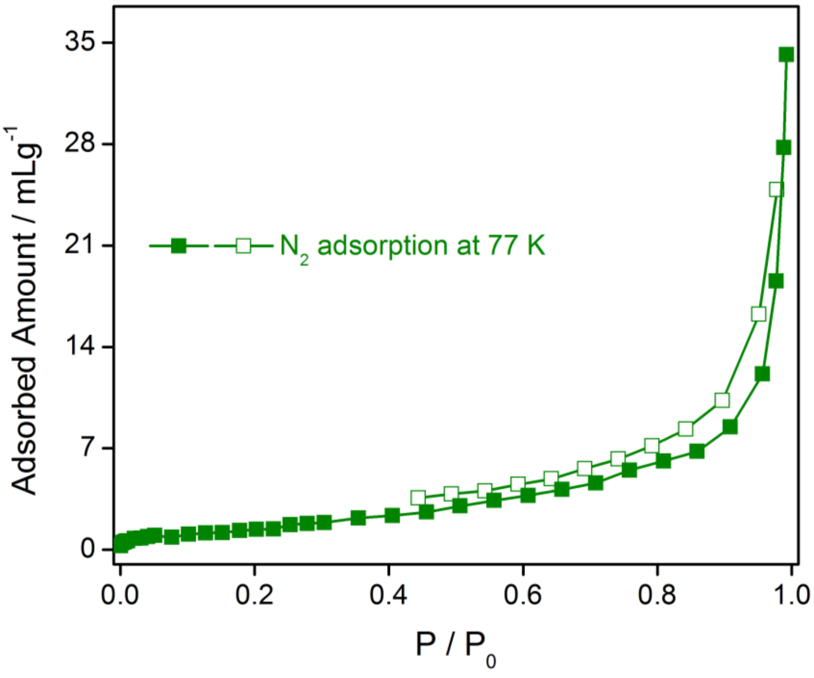

Figure S3: Low temperature (77 K) N_2 adsorption profile of compound-1.

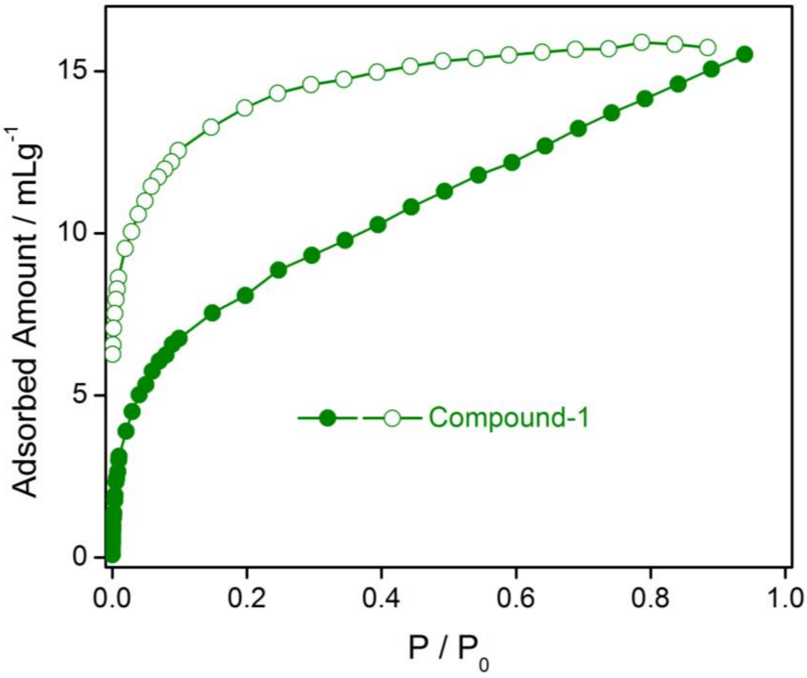

Figure S4: Low temperature (195 K) CO_2 adsorption profile of compound-1.

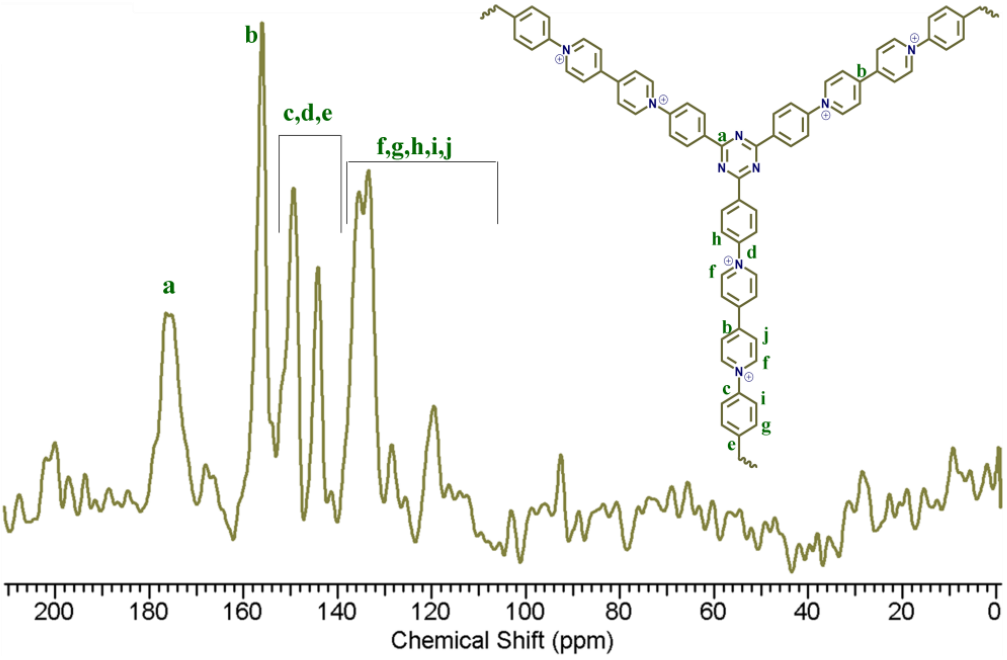

Figure S5: Solid state ^{13}C-NMR of compound-1.

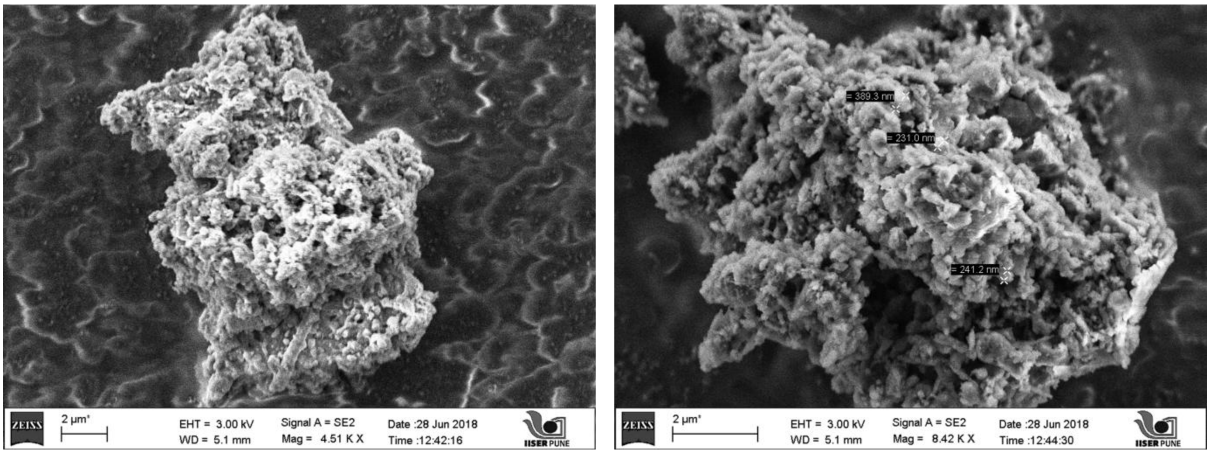

Figure S6: FESEM images of compound-1.

Element	Weight %
C	73.08
N	6.46
O	17.61
Cl	2.85
Total	100

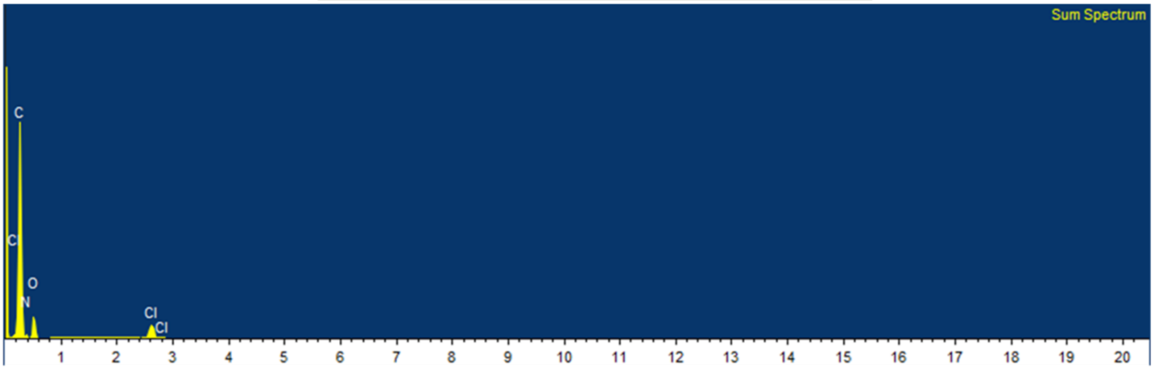

Figure S7: EDX analysis of compound-1.

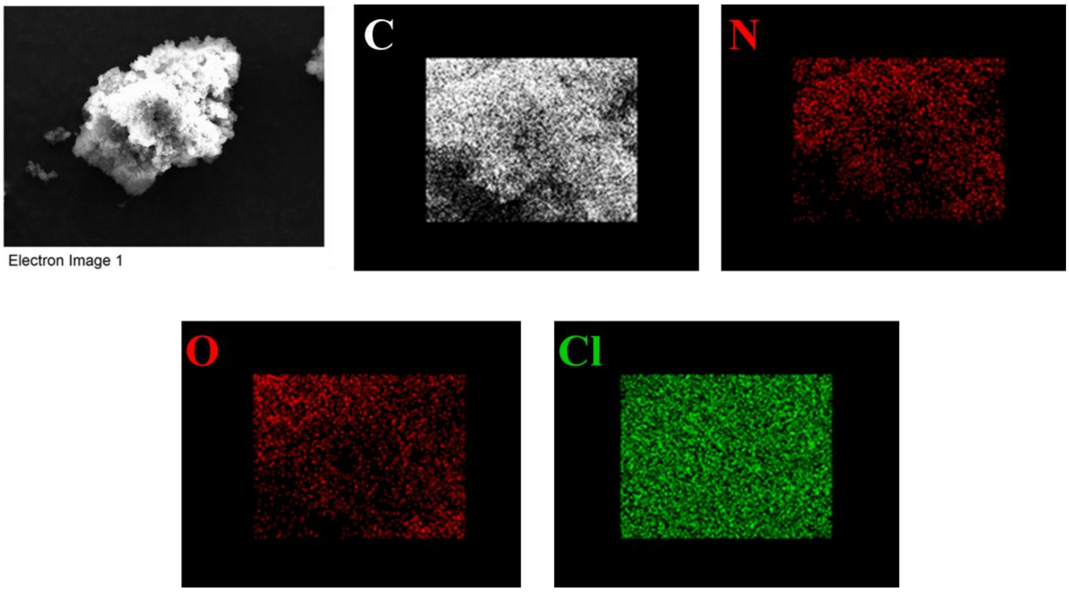

Figure S8: Elemental mapping of compound-1.

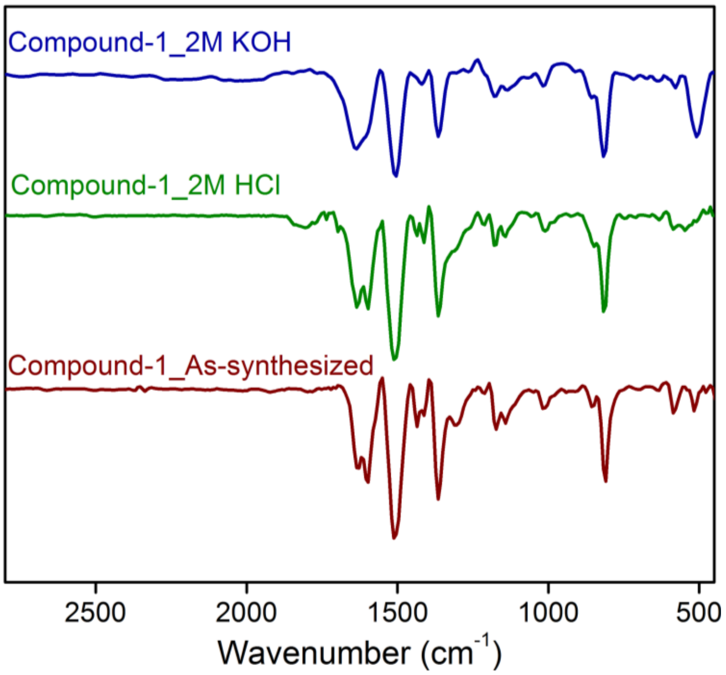

Figure S9: Infra-red (IR) spectroscopy of compound-1 (wine red), 2 M HCl treated compound-1 (green) and 2 M KOH treated compound-1 (blue).

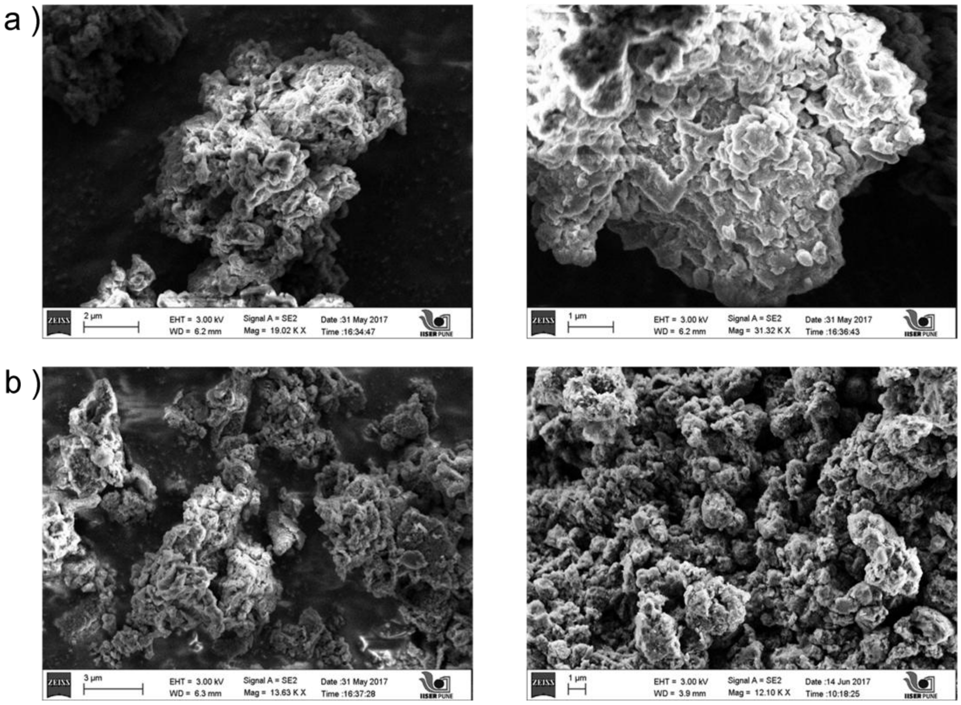

Figure S10: FESEM images of a) 2 M HCl treated compound-1 and b) 2 M KOH treated compound-1.

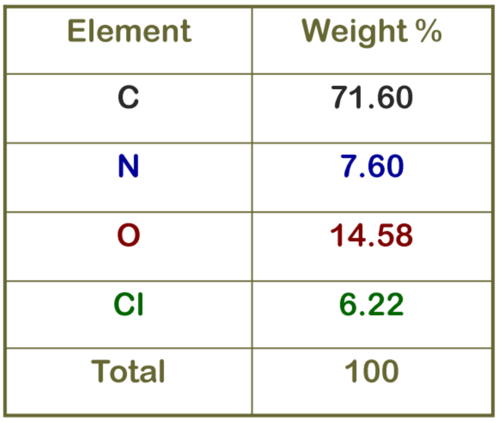

Element	Weight %
C	71.60
N	7.60
O	14.58
Cl	6.22
Total	100

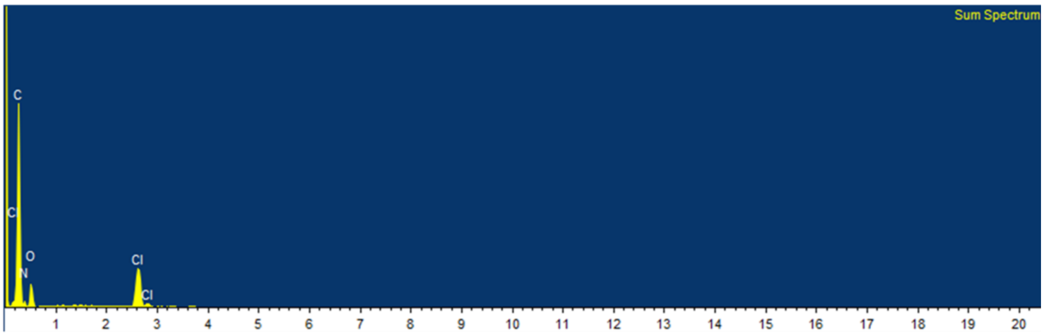

Figure S11: EDX analysis of 2 M HCl treated compound-1.

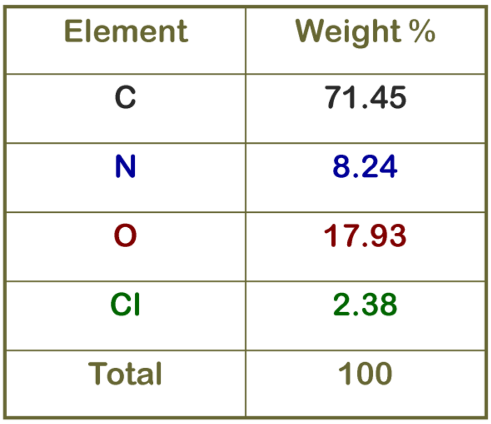

Element	Weight %
C	71.45
N	8.24
O	17.93
Cl	2.38
Total	100

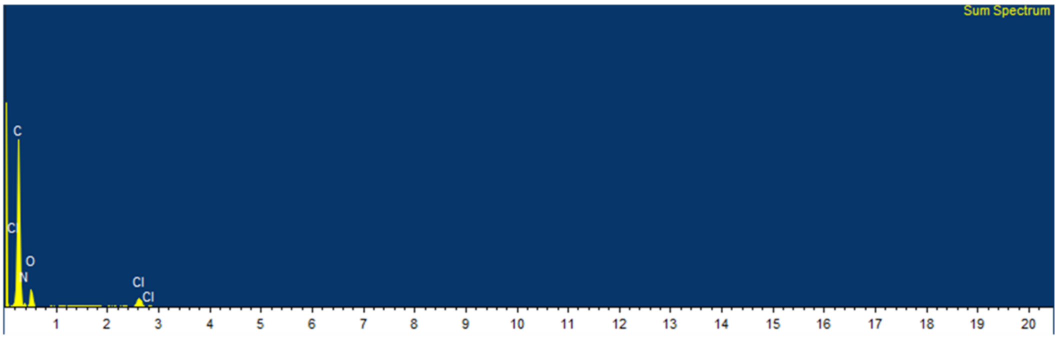

Figure S12: EDX analysis of 2 M KOH treated compound-1.

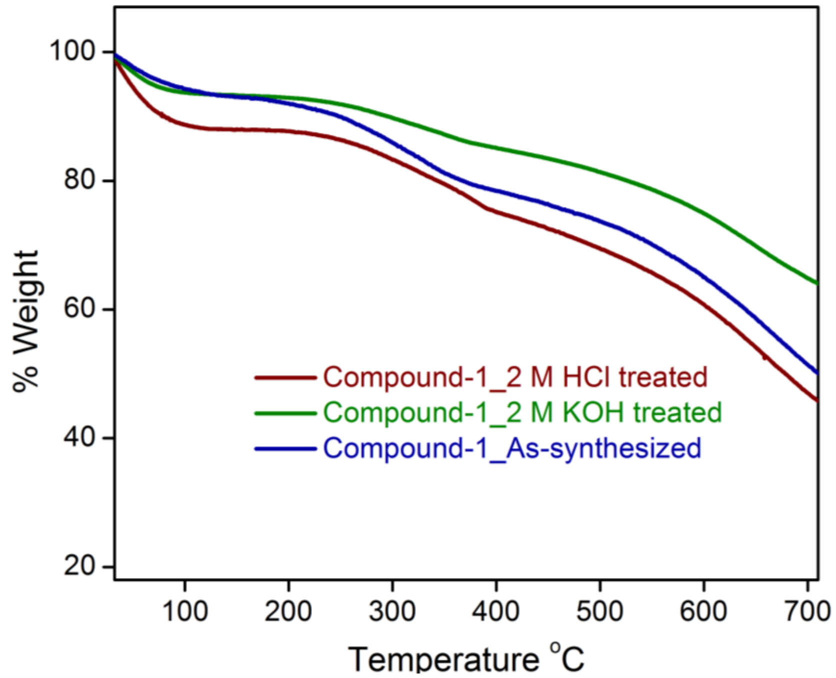

Figure S13: Thermogravimetric analysis (TGA) of compound-1 (blue), 2 M HCl treated compound-1 (wine red) and 2 M KOH treated compound-1 (green).

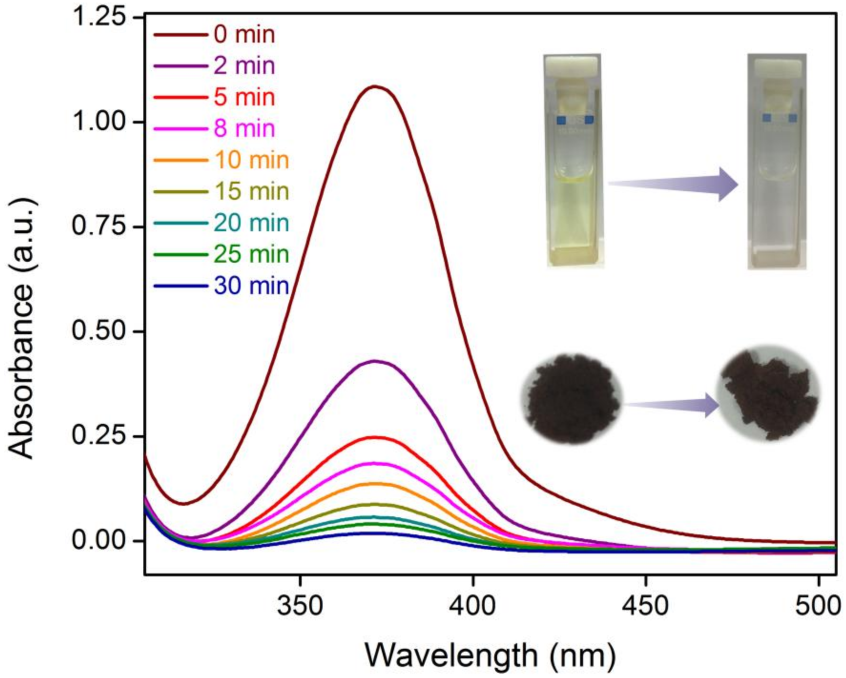

Figure S14: UV-Vis spectroscopy of CrO_4^{2-} ion solution in water in presence of compound-1 at different time intervals (Inset: images of CrO_4^{2-} ion solution and solid compound-1 before and after of capture study).

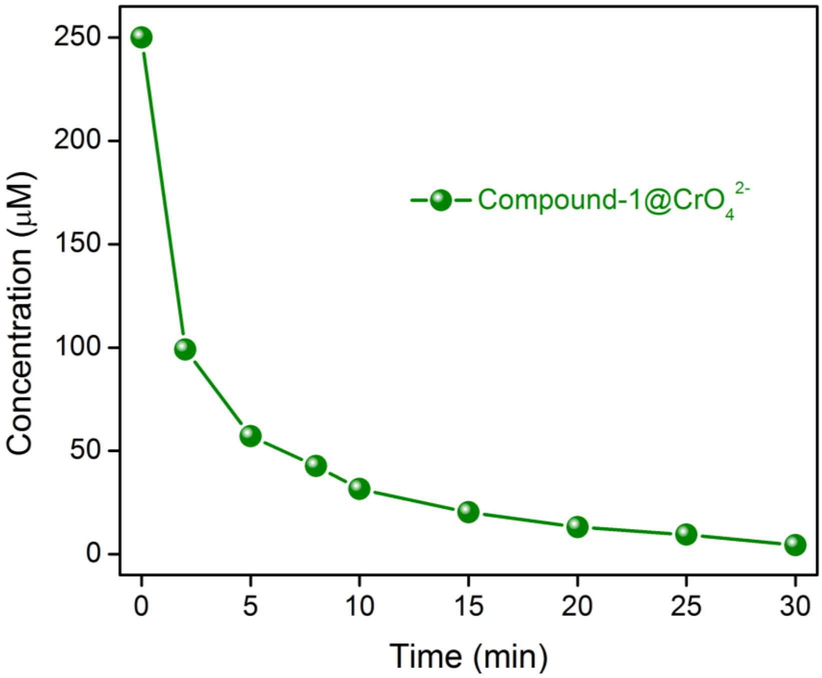

Figure S15: Decrease in the concentration of the CrO_4^{2-} ion from water after addition of compound-1.

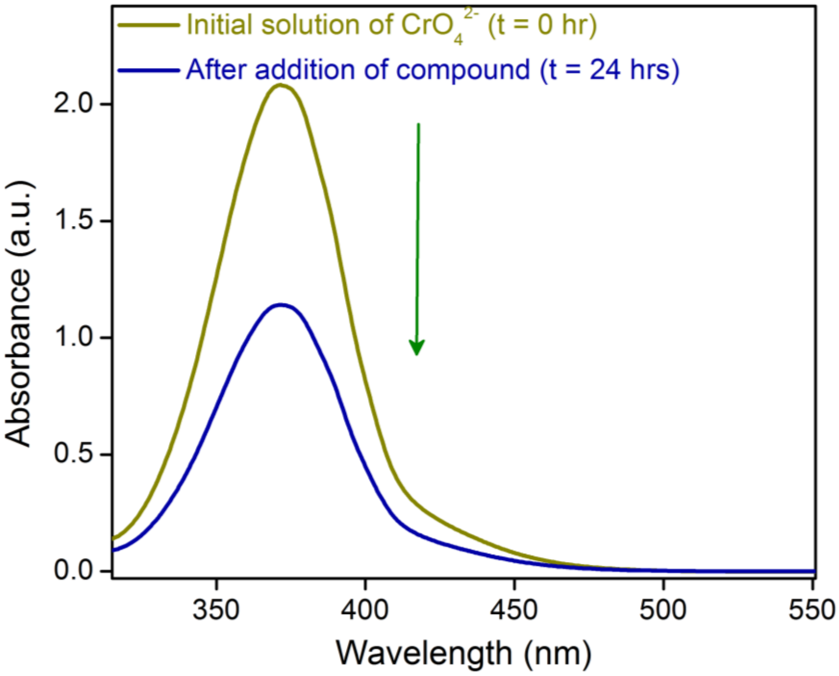

Figure S16: UV-Vis spectra of only CrO_4^{2-} before (dark yellow) and after (blue) addition of compound-1 (time duration: 24hrs); capacity of compound-1 for CrO_4^{2-} ion has been calculated from this data.

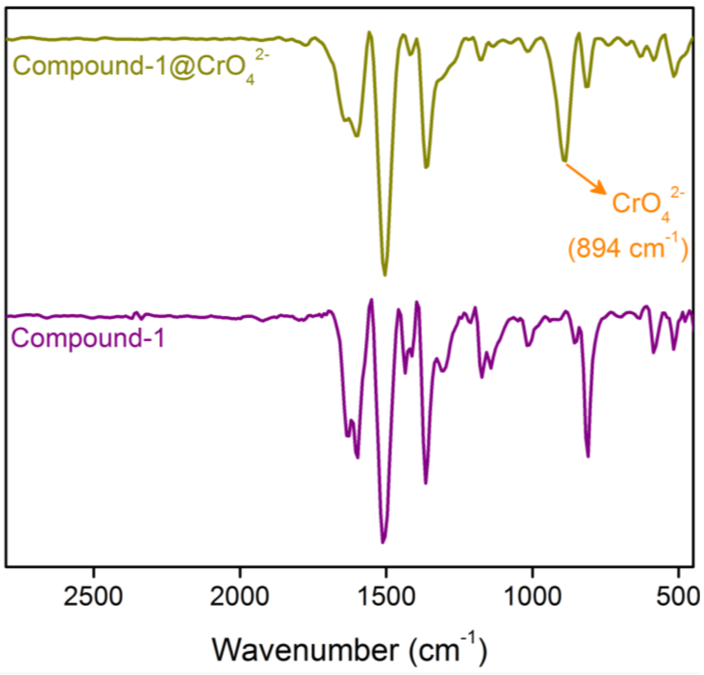

Figure S17: Infra-red (IR) spectroscopy of compound-1 (purple) and compound-$1\supset\mathrm{CrO_4^{2-}}$ (dark yellow).

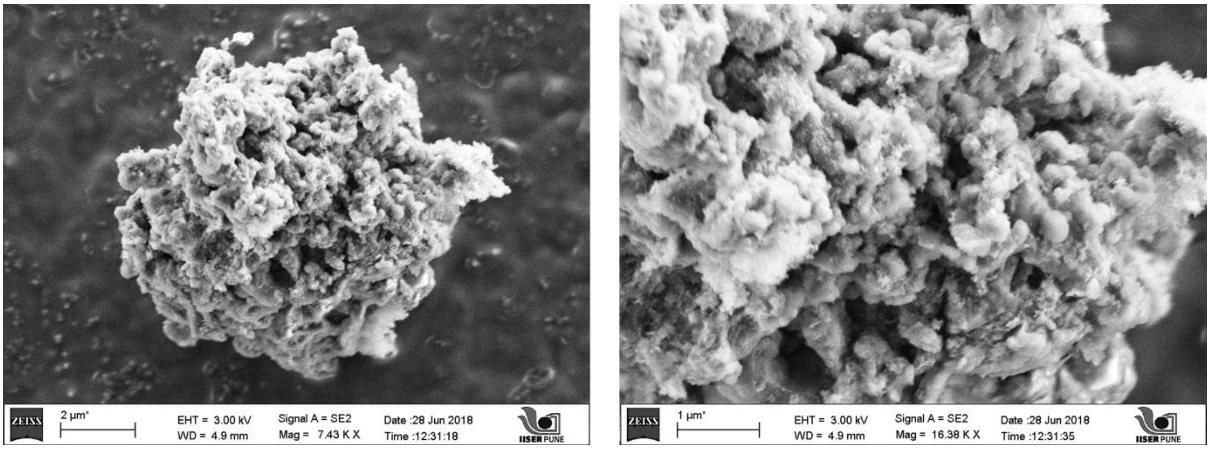

Figure S18: SEM images of $\mathrm{CrO_4^{2-}}$ encapsulated compound-1 (compound-$1\supset\mathrm{CrO_4^{2-}}$).

Element	Weight %
C	58.10
N	15.96
O	19.33
Cr	6.61
Total	100

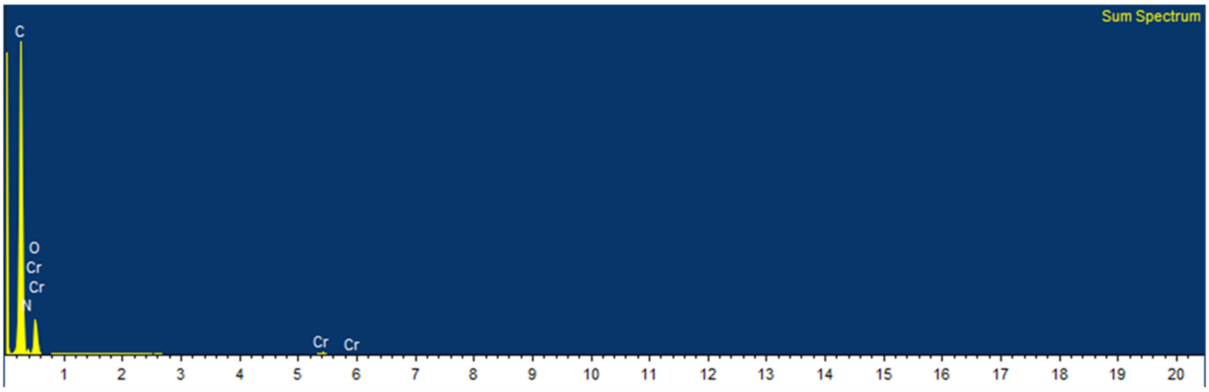

Figure S19: EDX analysis of CrO$_4^{2-}$ encapsulated compound-1 (compound-1$\supset$CrO$_4^{2-}$).

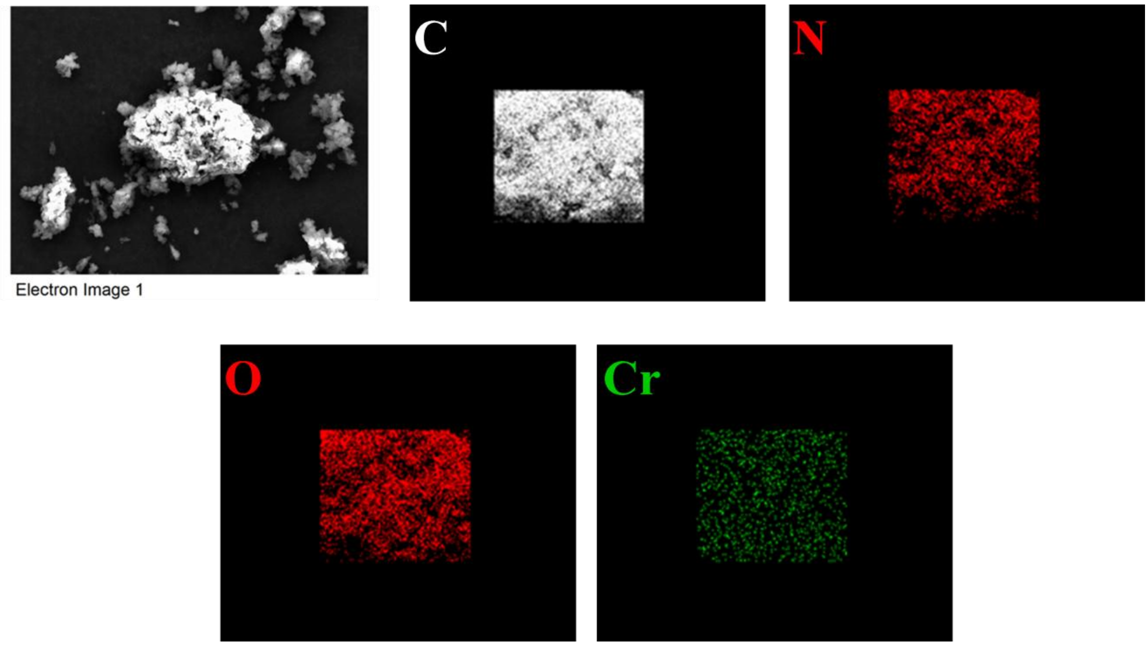

Figure S20: Elemental mapping of CrO$_4^{2-}$ encapsulated compound-1 (compound-1$\supset$CrO$_4^{2-}$).

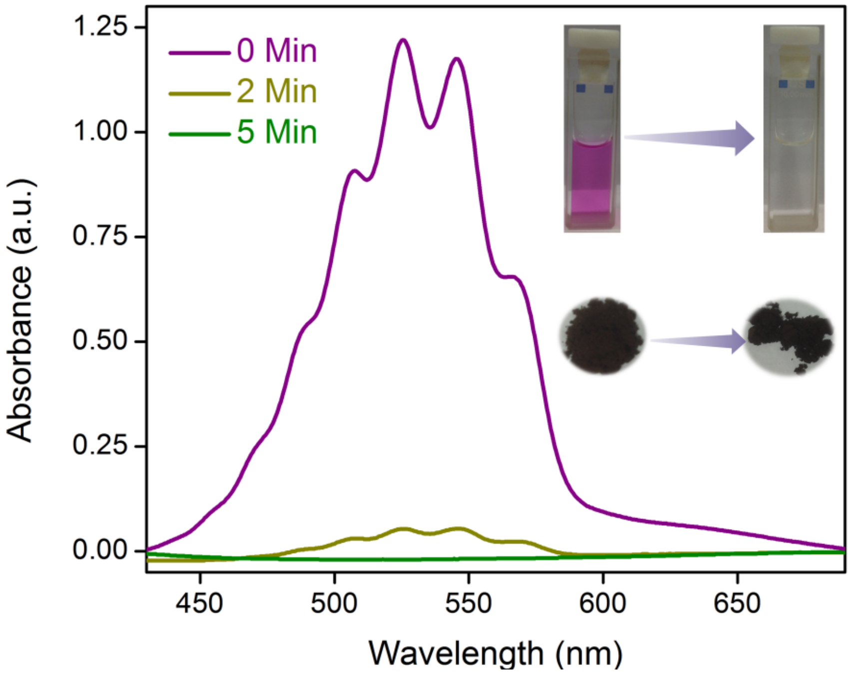

Figure S21: UV-Vis spectroscopy of MnO_4^- ion solution in water in presence of compound-1 at different time intervals (Inset: images of MnO_4^- ion solution and solid compound-1 before and after of capture study).

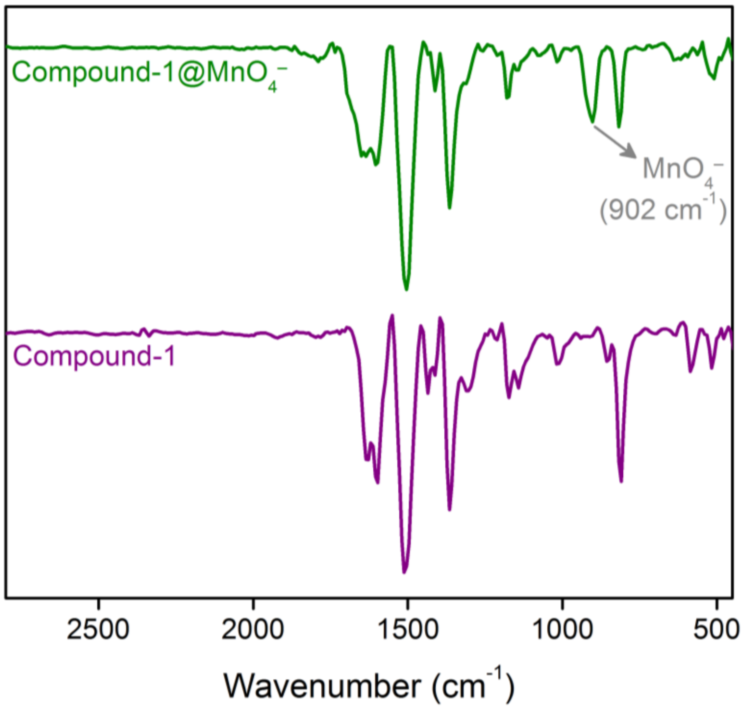

Figure S22: Infra-red (IR) spectroscopy of compound-1 (purple) and compound-1$\supset MnO_4^-$ (green).

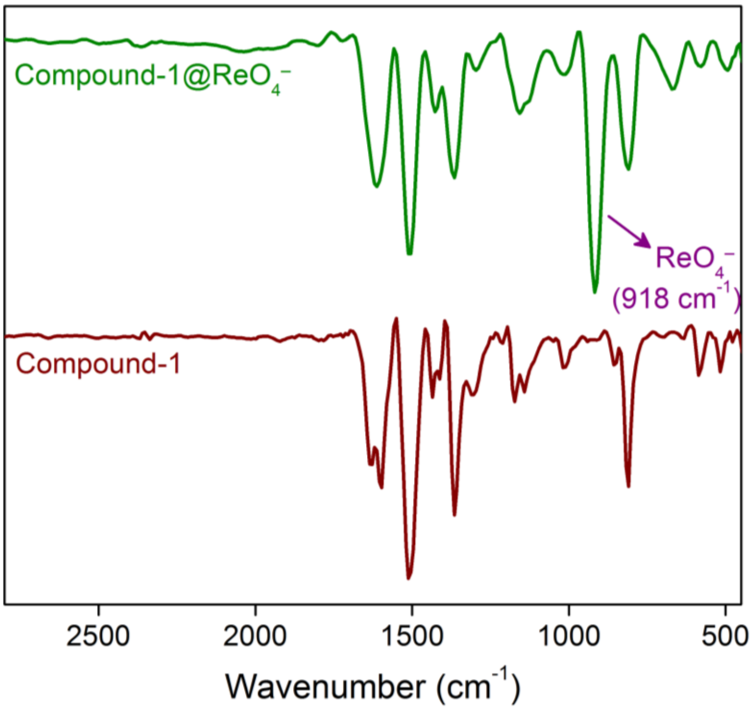

Figure S23: IR spectra of compound-1 (wine red) and ReO$_4^-$ treated compound-1 (green).

Element	Weight %
C	61.01
N	13.87
O	15.22
Mn	9.90
Total	100

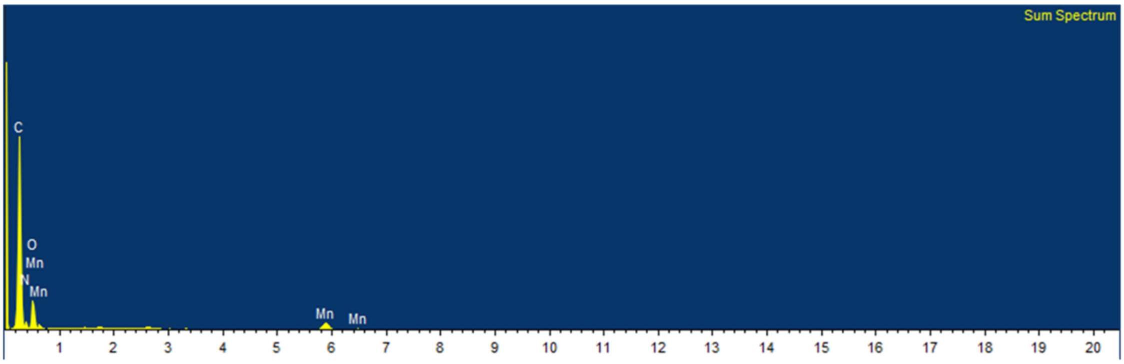

Figure S24: EDX analysis of MnO$_4^-$ encapsulated compound-1 (compound-1$\supset$MnO$_4^-$).

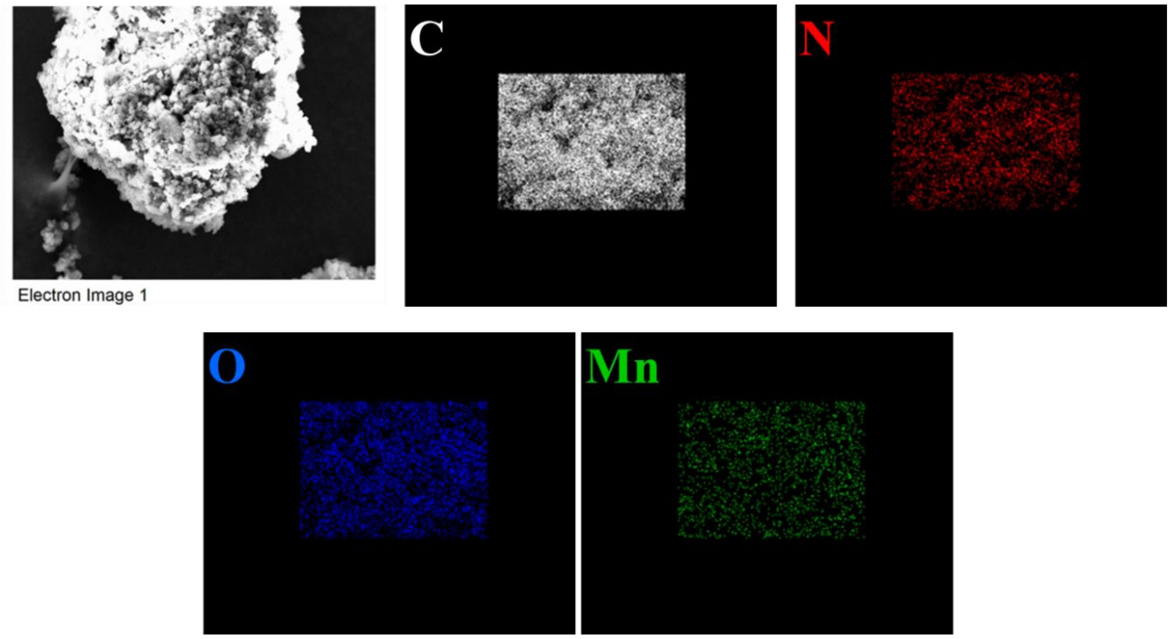

Figure S25: Elemental mapping of MnO_4^- encapsulated compound-1 (compound-1$\supset$$MnO_4^-$).

Element	Weight %
C	69.23
N	3.63
O	21.82
Re	5.32
Total	100

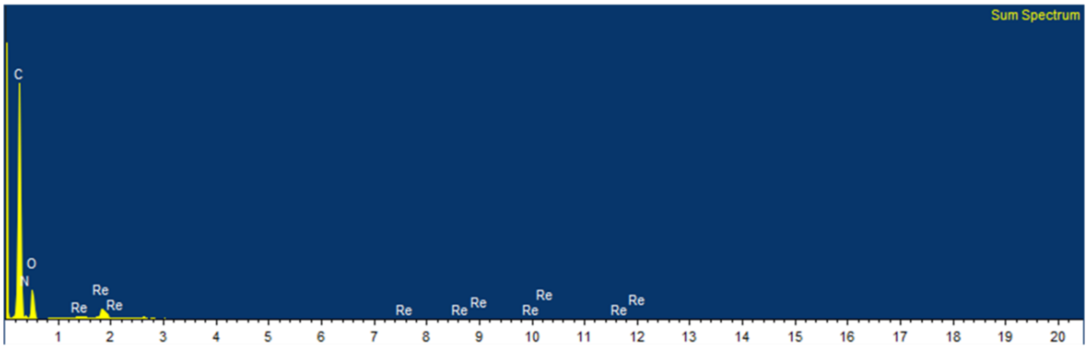

Figure S26: EDX analysis of compound-1 after the capture of ReO_4^-.

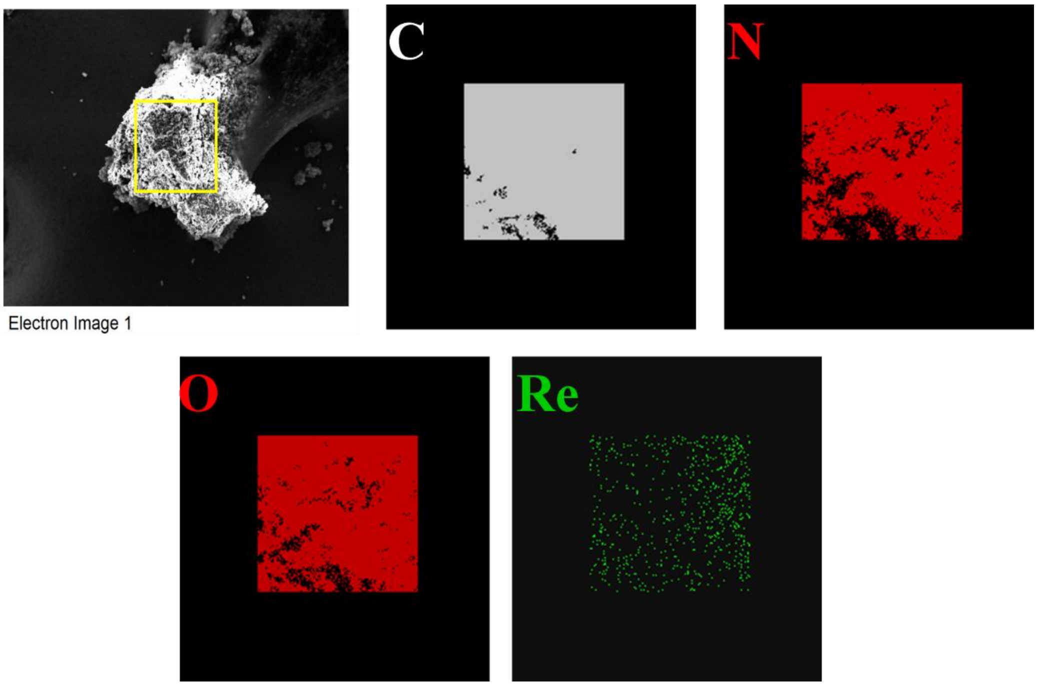

Figure S27: Elemental mapping of compound-1 after the capture of ReO$_4^-$.

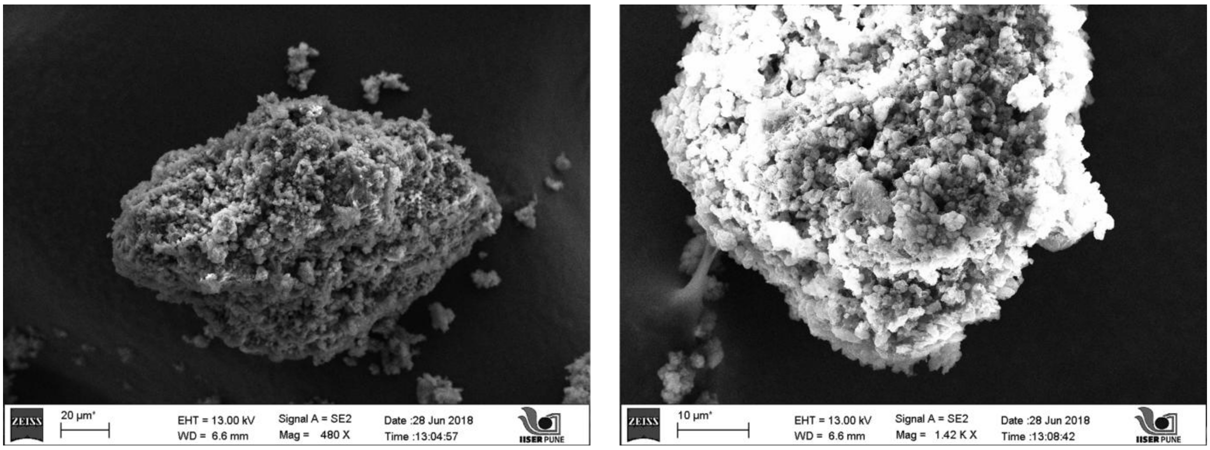

Figure S28: SEM images of MnO$_4^-$ encapsulated compound-1 (compound-1⊃ MnO$_4^-$).

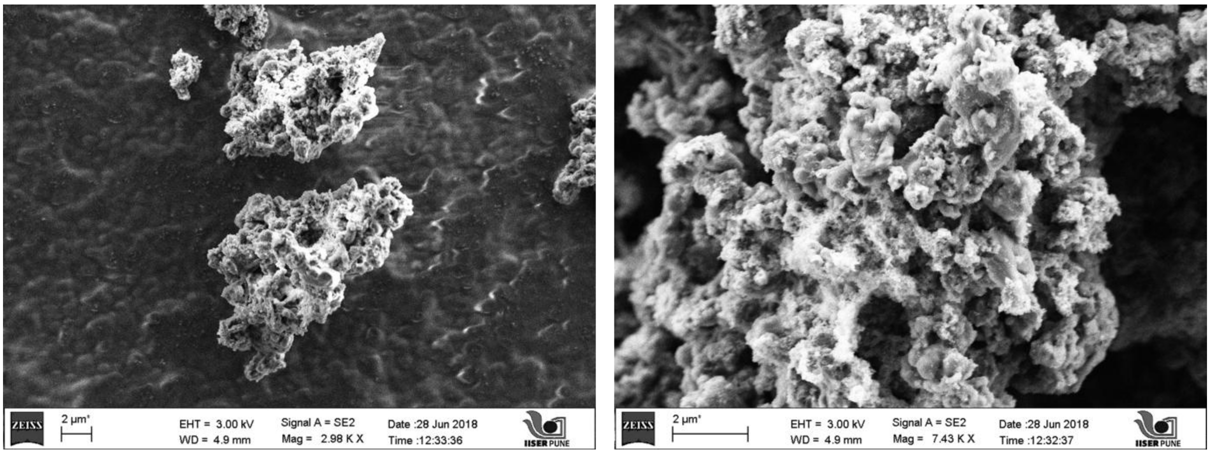

Figure S29: SEM images of compound-1 after the treatment of ReO_4^- in water medium.

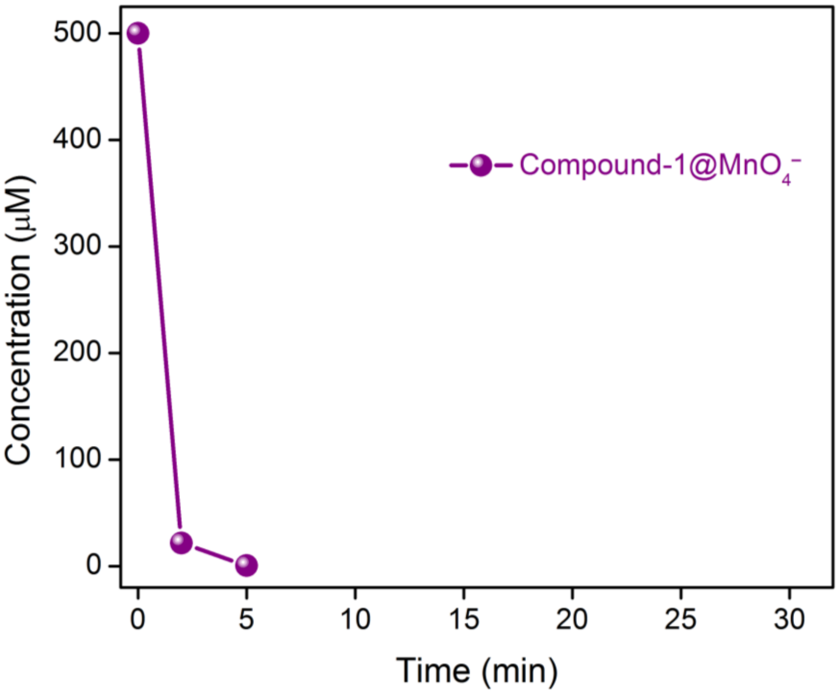

Figure S30: Decrease in the concentration of the MnO_4^- ion from water after addition of compound-1.

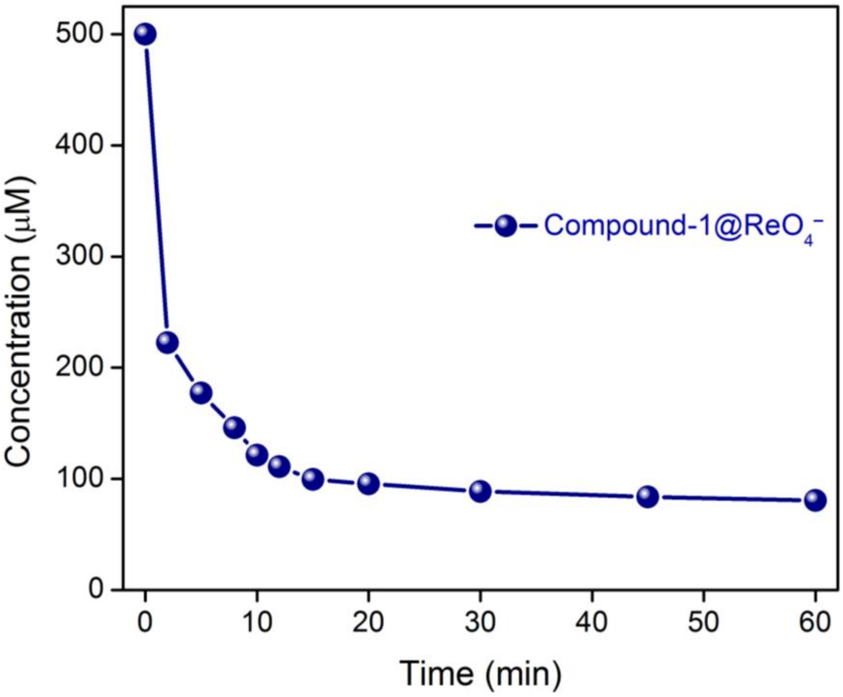

Figure S31: Decrease in the concentration of the ReO_4^- ion from water solution on addition of compound-1.

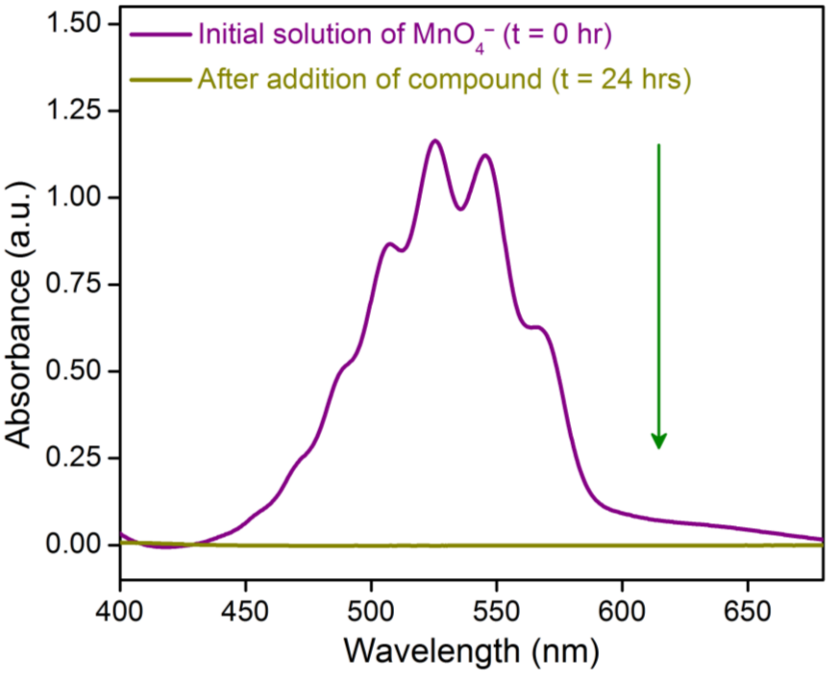

Figure S32: UV-Vis spectra of only MnO_4^- before (purple) and after (dark yellow) addition of compound-1 (time duration = 24hrs); capacity of compound-1 for MnO_4^- ion has been calculated from this data.

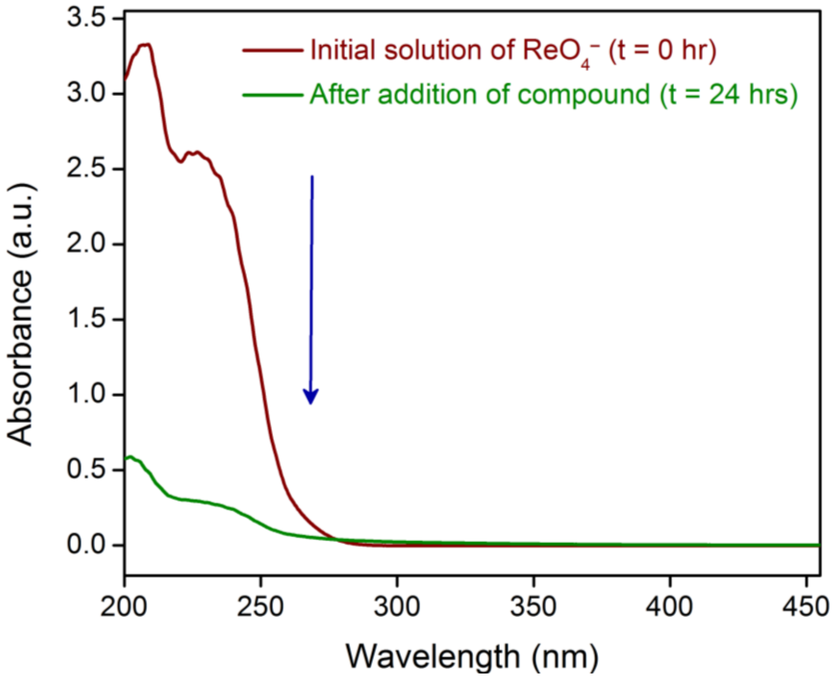

Figure S33: UV-Vis spectra of only ReO$_4^-$ before (wine red) and after (green) the addition of compound-1 (time duration = 24hrs); capacity of compound-1 for ReO$_4^-$ ion has been calculated from this data.

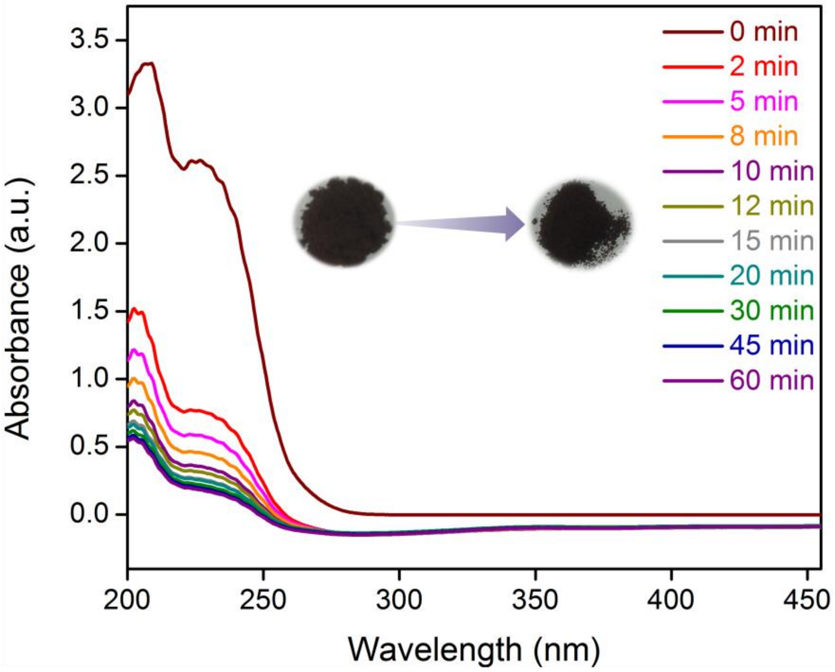

Figure S34: UV-Vis spectroscopy of ReO$_4^-$ ion solution in water in presence of compound-1 at different time intervals (Inset: images of ReO$_4^-$ ion solution and solid compound-1 before and after of capture study).

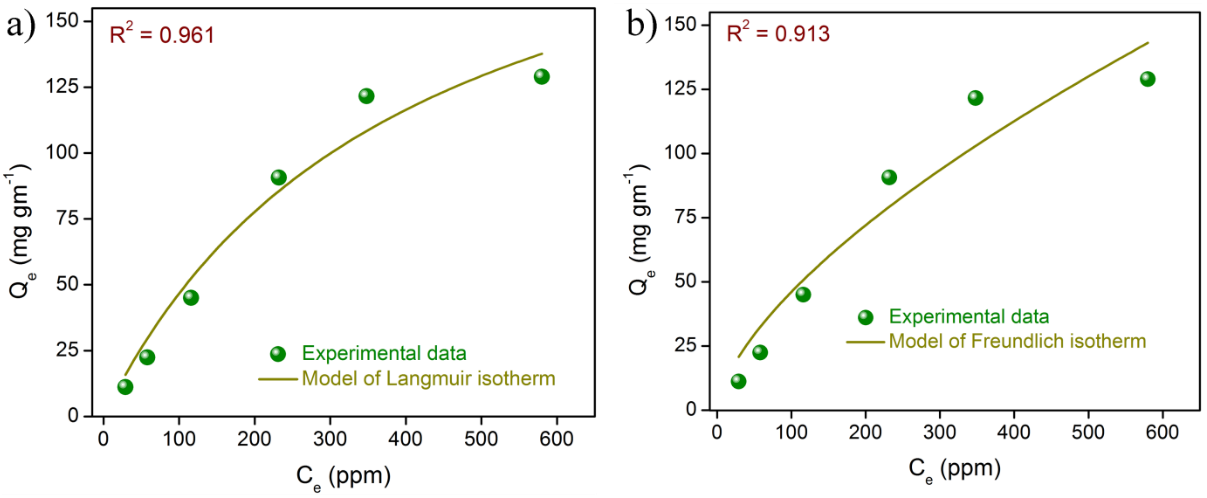

Figure S35: (a) Langmuir model and (b) Freundlich model of CrO_4^{2-} ion capture study with compound-1.

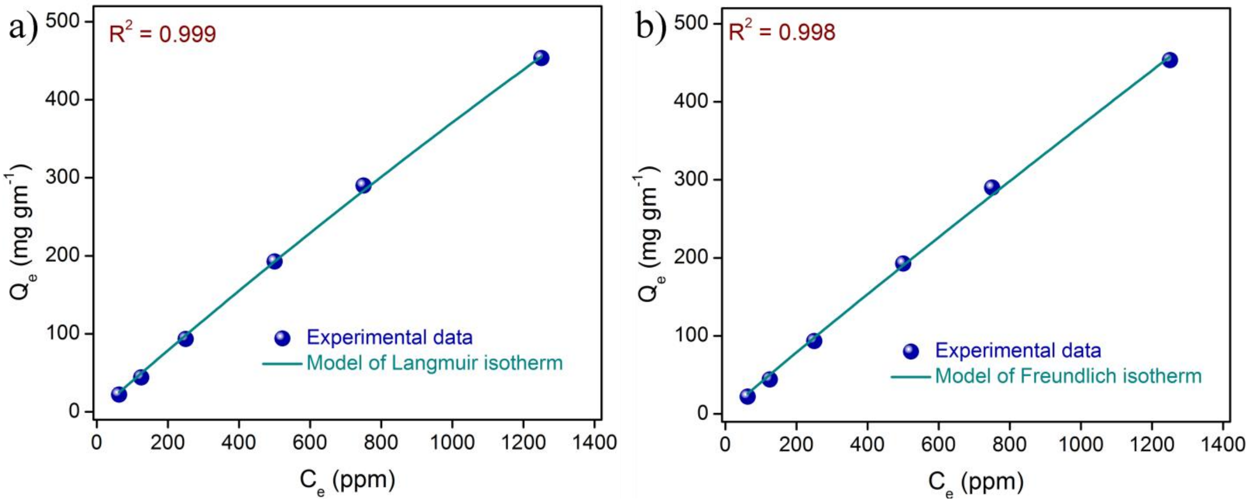

Figure S36: (a) Langmuir model and (b) Freundlich model of ReO_4^- ion capture study with compound-1.

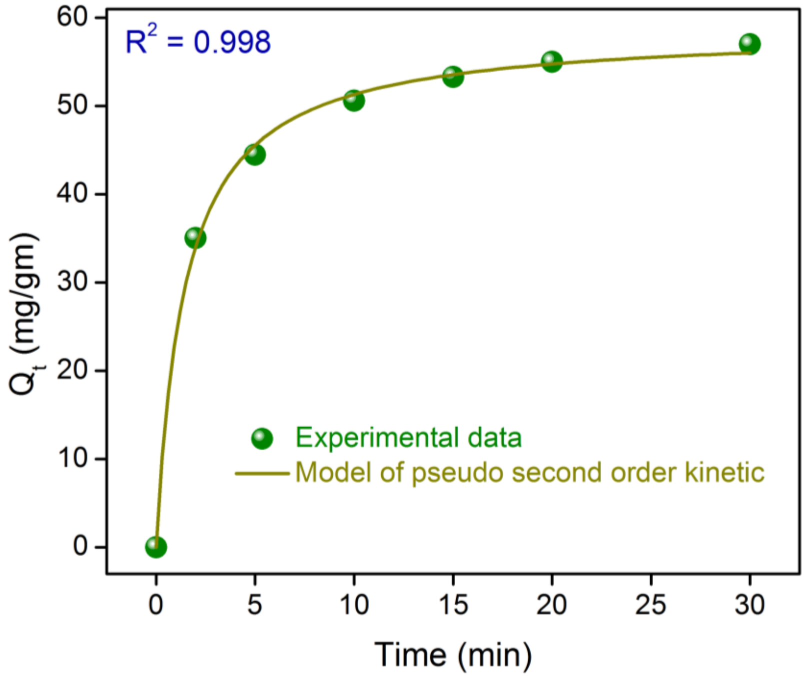

Figure S37: Kinetic study of CrO_4^{2-} ion capture with compound-1.

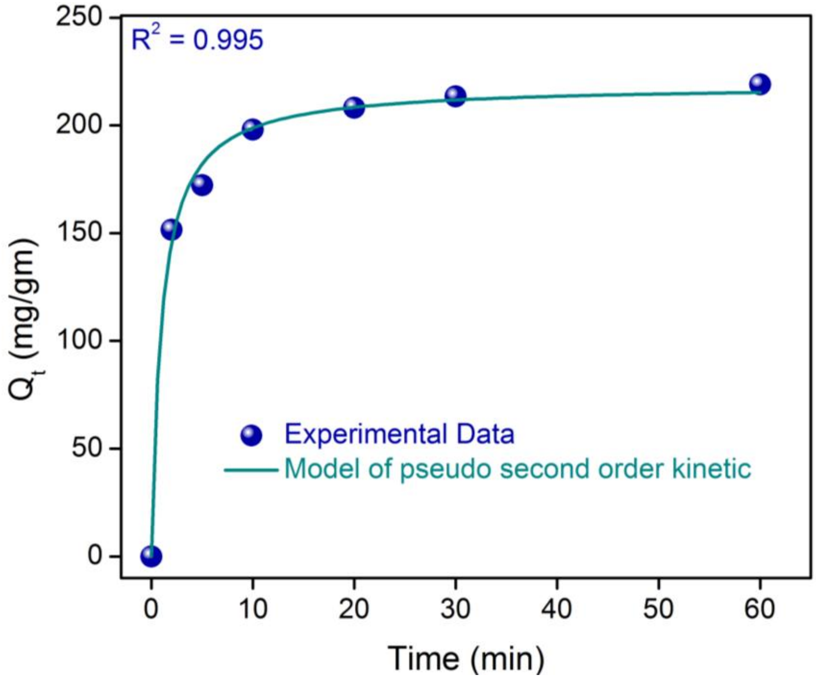

Figure S38: Kinetic study of ReO_4^- ion capture with compound-1.

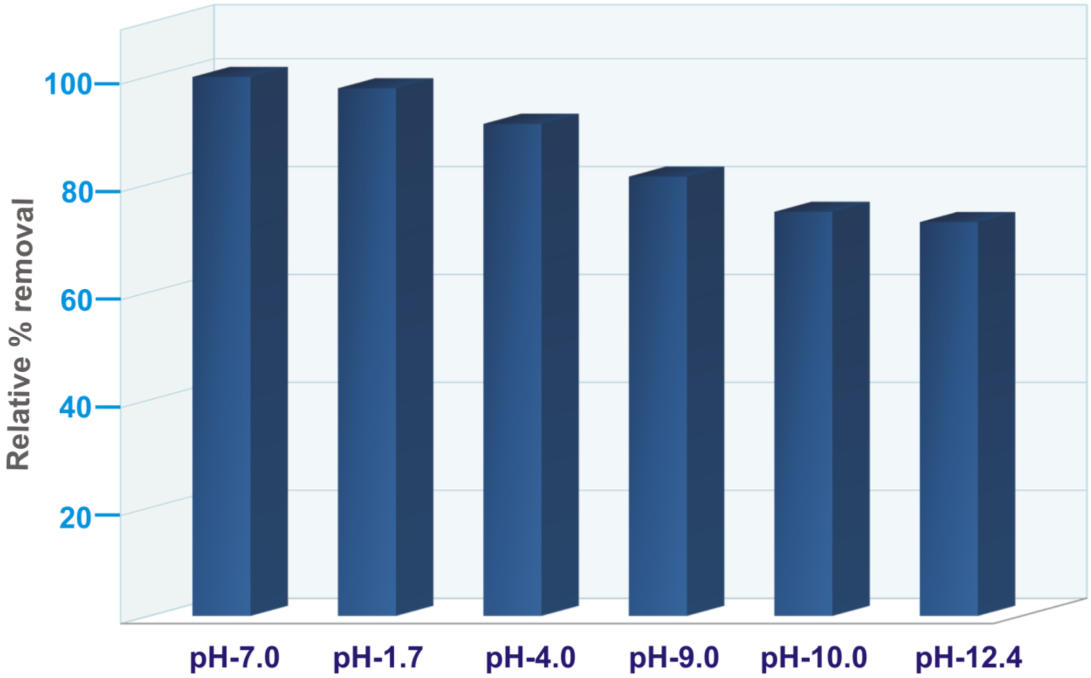

Figure S39: Bar diagram representing relative % removal of CrO_4^{2-} ion from water by compound-1 at different pH-medium.

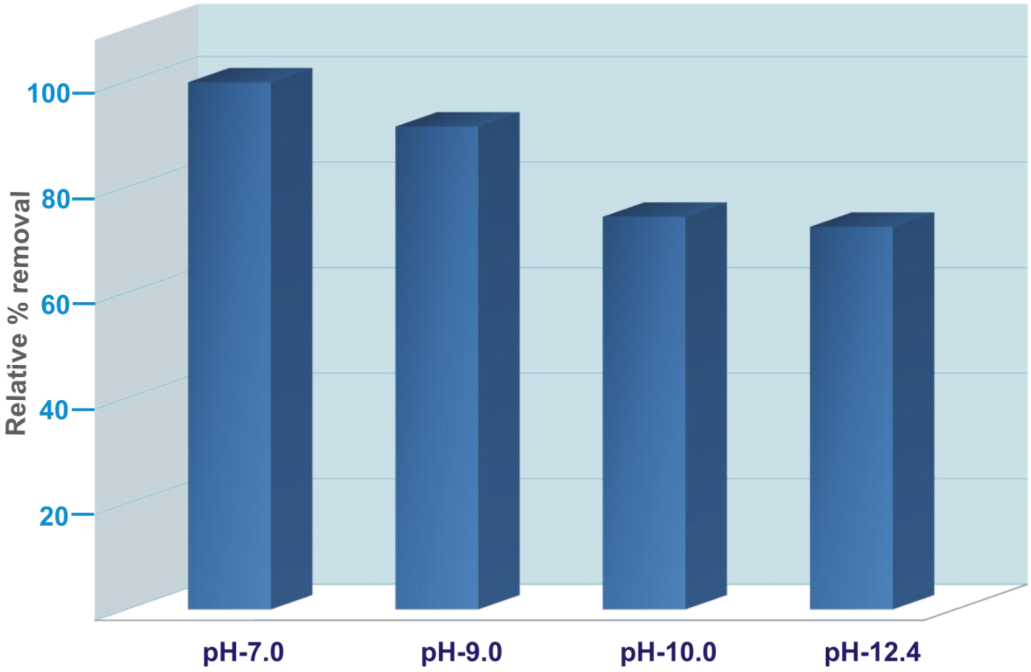

Figure S40: Bar diagram representing relative % removal of ReO_4^- ion from water by compound-1 at different alkaline pH-medium.

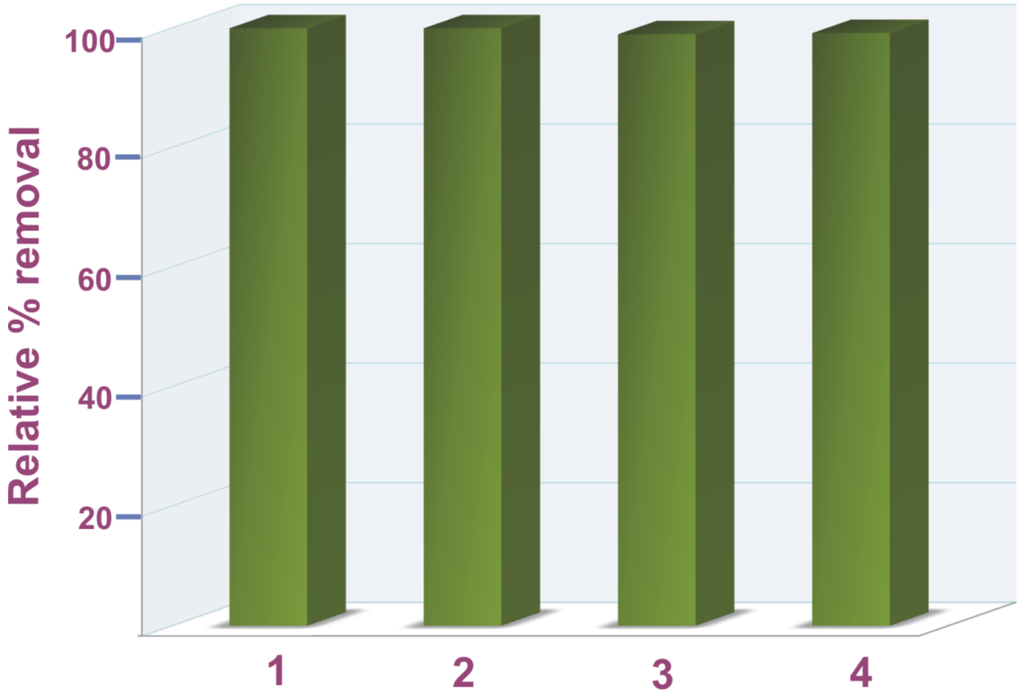

Figure S41: Recyclability test of compound-1 for CrO_4^{2-} ion.

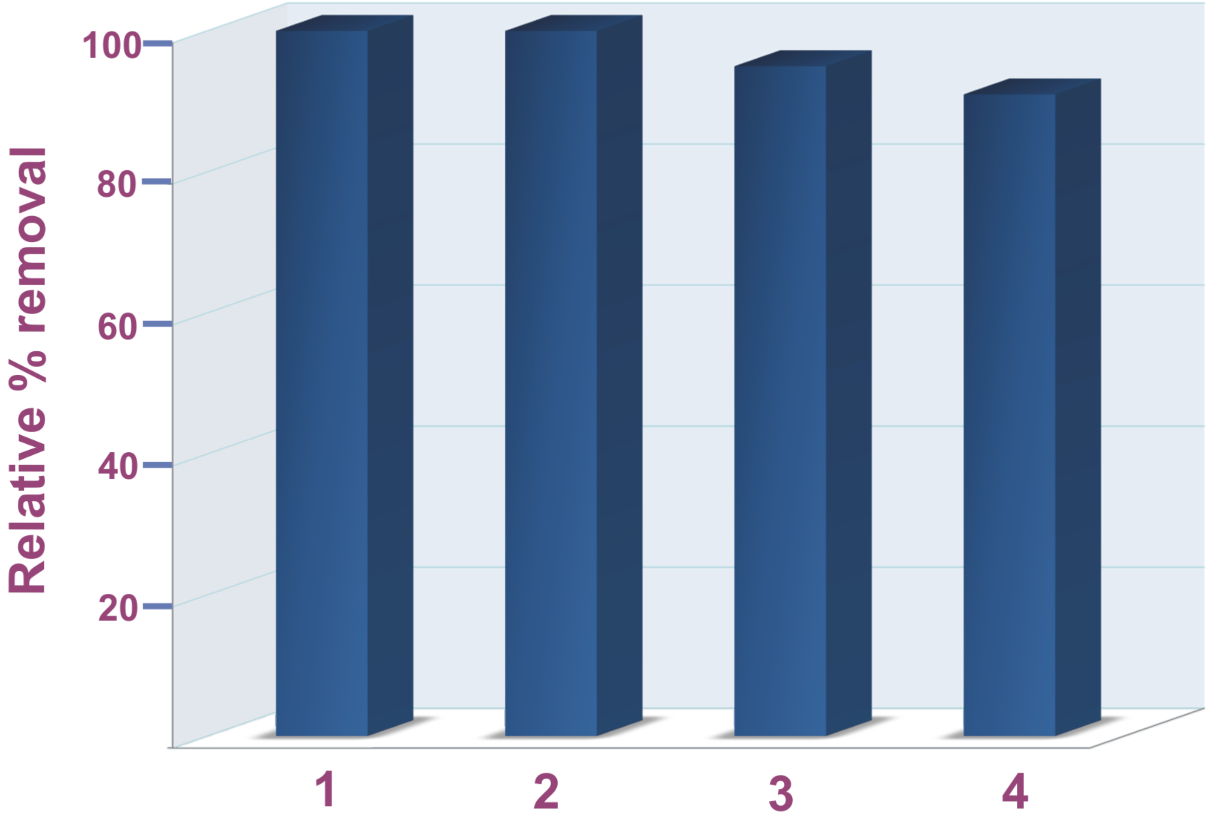

Figure S42: Recycle test of compound-1 for ReO_4^- ion.

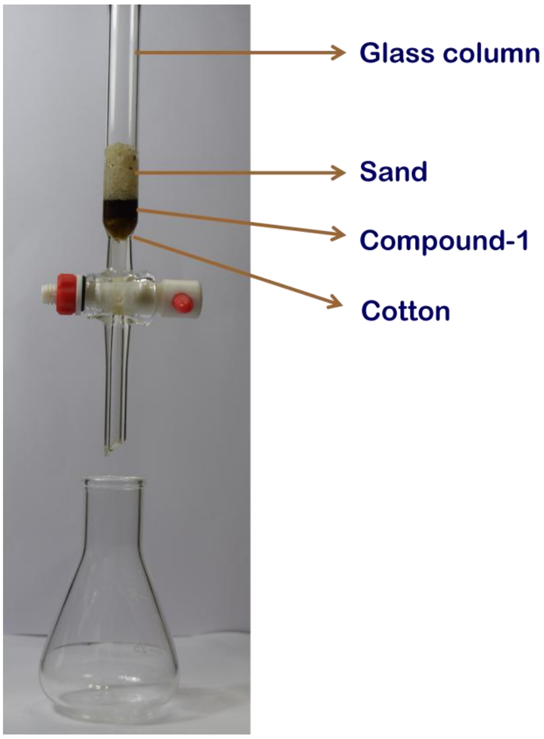

Figure S43: Representation of the compound-1 loaded column used for column chromatographic separation of oxo-anion from water.

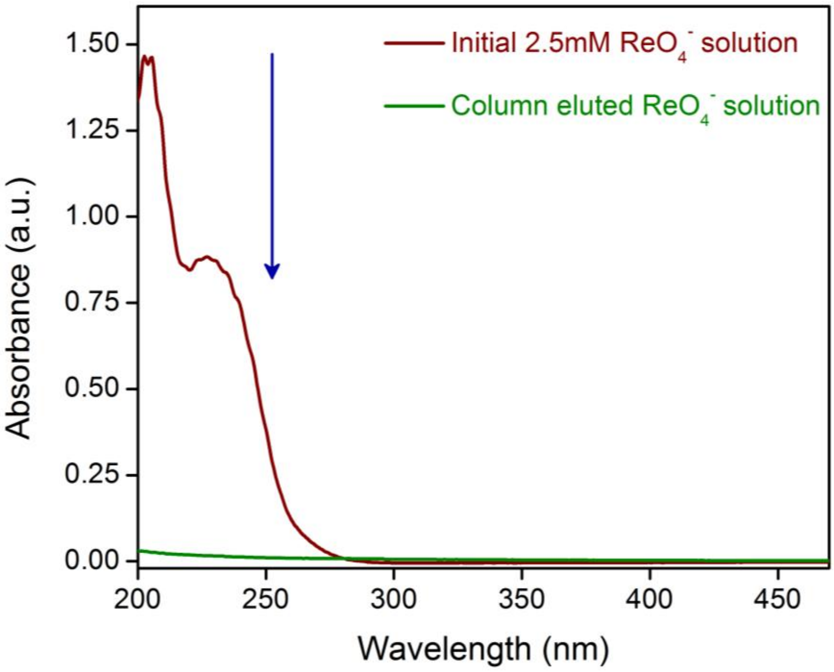

Figure S44: UV-Vis spectra of the 2.5 mM ReO_4^- solution before (wine red) and after (green) passing through the compound-1 loaded column.

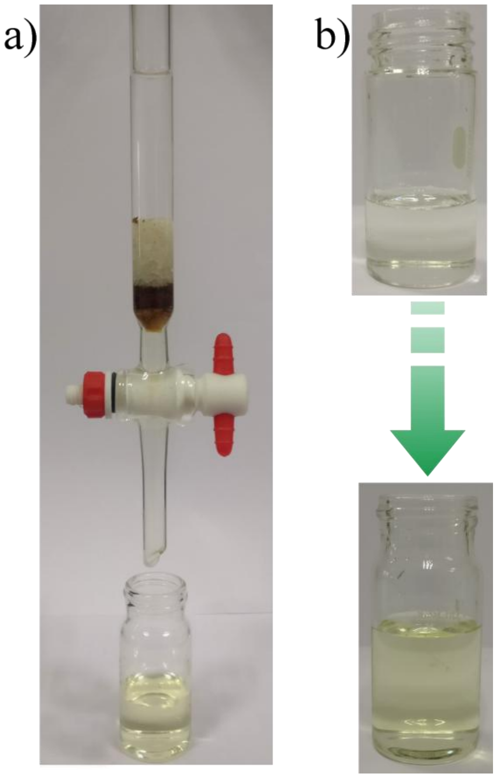

Figure S45: (a) Regeneration of the column with 3 M HCl solution; (b) images of HCl solution before (top) and after (bottom) passing through the column.

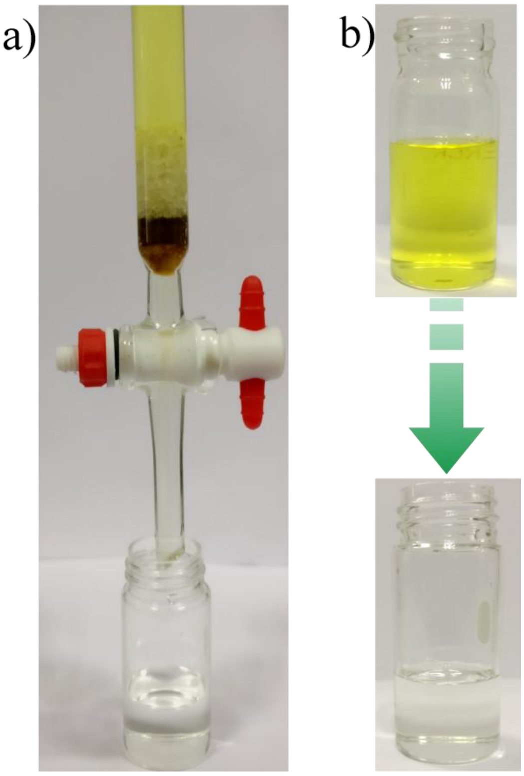

Figure S46: (a) Recyclability test with the regenerated column; (b) images of CrO_4^{2-} solution (top) and after (bottom) passing through the column.

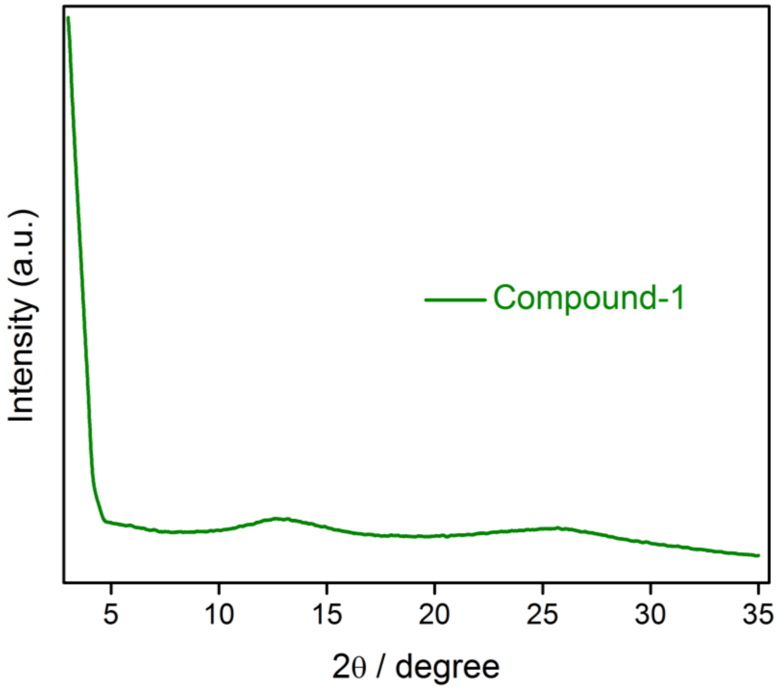

Figure S47: Powder X-ray diffraction (PXRD) pattern of compound-1.

Table S1: A comparison table of CrO_4^{2-} capture (CrO_4^{2-} mg/gm) with some well-studied examples in the literature (N.D.: Not done)

Compound	Capacity (mg/gm)	Selectivity	Reference
Compound-1	133	Cl^-, NO_3^-, Br^-, SO_4^{2-}	This work
Carbon nanocomposites	3.74	N.D.	1
Polyaniline	18.1	N.D.	2
MOR-2	263	Cl^-, NO_3^-, HCO_3^-, etc.	3
SLUG-21	60	NO_3^-, CO_3^{2-}	4
1-ClO_4	62.9	halide anions	5
1-NO_3	82.5	NO_3^-, CO_3^{2-}	6
Fe nanoparticles	109	N.D.	7
Zn–Co-SLUG-35	68.5	NO_3^-, SO_4^{2-}	8
TJU-1	279	Cl^-, HCO_3^-, NO_3^-, SO_4^{2-}	9
MgAl-LDHs	112	N.D.	10
ED-rGO	100	N.D.	11
ZIF-67	5.88-13.34	N.D.	12

Table S2: A comparison table of ReO_4^- and MnO_4^- capture (mg/gm) with some well-studied examples in the literature

Element	Compound	Capacity (mg/gm)	Selectivity	Reference
ReO_4^-	Compound-1	517	Cl^-, NO_3^-, Br^-, SO_4^{2-}	This Work
MnO_4^-	Compound-1	297.3	Cl^-, NO_3^-, Br^-, SO_4^{2-}	This Work
ReO_4^-	D318 resin	351	-	13
ReO_4^-	PAF-1-F	420	SO_4^{2-}, PO_4^{3-}	14
ReO_4^-	Dowex1x8	98.1	-	14
ReO_4^-	Purolite 530E	96	-	14
ReO_4^-	SLUG-21	602	-	15
ReO_4^-	UiO-66-NH_3^+	159	NO_3^-, SO_4^{2-}, PO_4^{3-}	16
ReO_4^-	SCU-100	541	CO_3^{2-}, SO_4^{2-}, PO_4^{3-}	17
ReO_4^-	SCU-101	217	various anions	18
ReO_4^-	PolyDMAEMA hydrogels	30.5	-	19
ReO_4^-	4-ATR resin	354		20
ReO_4^-	SBN	786	-	21
ReO_4^-	LDHs	130	-	21
MnO_4^-	SLUG-21	283	NO_3^-, CO_3^{2-}	15

References:

[1] J. Zhu, S. Wei, H. Gu, S. B. Rapole, Q. Wang, Z. Luo, N. Haldolaarachchige, D. P. Young, Z. Guo, *Environ. Sci. Technol.* **2012**, *46*, 977‑985.

[2] B. Qiu, C. Xu, D. Sun, H. Wei, X. Zhang, J. Guo, Q. Wang, D. Rutman, Z. Guo, S. Wei, *RSC Adv.* **2014**, *4*, 29855‑29865.

[3] S. Rapti, D. Sarma, S. A. Diamantis, E. Skliri, G. S. Armatas, A. C. Tsipis, Y. S. Hassan, M. Alkordi, C. D. Malliakas, M. G. Kanatzidis, T. Lazarides, J. C. Plakatouras, M. J. Manos, *J. Mater. Chem. A* **2017**, *5*, 14707–14719.

[4] H. Fei, M. R. Bresler, S. R. J. Oliver, *J. Am. Chem. Soc.* **2011**, *133*, 11110−11113.

[5] P. Shi, B. Zhao, G. Xiong, Y. Hou, P. Cheng, *Chem. Commun.* **2012**, *48*, 8231−8233.

[6] L. Li, X. Feng, R. Han, S. Zang, G. Yang, *J. Hazard. Mater.* **2017**, *321*, 622−628.

[7] J. Cao, W. -X. Zhang, *J. Hazard. Mater.* **2006**, *132*, 213−219.

[8] H. Fei, C. S. Han, J. C. Robins, S. R. J. Oliver, *Chem. Mater.* **2013**, *25*, 647−652.

[9] H. Yang, H. Fei, *Chem. Commun.* **2017**, *53*, 7064−7067.

[10] Y. Li, B. Gao, T. Wu, D. Sun, X. Li, B. Wang, F. Lu, *Water Res.* **2009**, *43*, 3067−3075.

[11] H. -L. Ma, Y. Zhang, Q. -H. Hu, D. Yan, Z. -Z. Yu, M. Zhai, *J. Mater. Chem.* **2012**, *22*, 5914−5916.

[12] X. Li, X. Gao, L. Ai, J. Jiang, *Chem. Eng. J.* **2015**, *274*, 238−246.

[13] Z. Shu, M. Yang, *Chinese. J. Chem. Eng.* **2010**, *18*, 372−376.

[14] D. Banerjee, S. K. Elsaidi, B. Aguila, B. Li, D. Kim, M. J. Schweiger, A. A. Kruger, C. J. Doonan, S. Ma, P. K. Thallapally, *Chem. Eur. J.* **2016**, *22*, 17581−17584.

[15] H. Fei, D. L. Rogow, S. R. J. Oliver, *J. Am. Chem. Soc.* **2010**, *132*, 7202−7209.

[16] D. Banerjee, W. Xu, Z. Nie, L. E. V. Johnson, C. Coghlan, M. L. Sushko, D. Kim, M. J. Schweiger, A. A. Kruger, C. J. Doonan, P. K. Thallapally, *Inorg. Chem.* **2016**, *55*, 8241−8243.

[17] D. Sheng, L. Zhu, C. Xu, C. Xiao, Y. Wang, Y. Wang, L. Chen, J. Diwu, J. Chen, Z. Chai, S. Wang, *Environ. Sci. Technol.* **2017**, *51*, 3471−3479.

[18] L. Zhu, V. Sheng, C. Xu, X. Dai, M. A. Silver, J. Li, P. Li, Y. Wang, Y. Wang, L. Chen, C. Xiao, J. Chen, R. Zhou, C. Zhang, O. K. Farha, Z. Chai, T. E. Albrecht-Schmitt, S. Wang, *J. Am. Chem. Soc.* **2017**, *139*, 14873‐14876.

[19] Y. Yan, M. Yi, M. L. Zhai, H. F. Ha, Z. F. Luo, X. Q. Xiang, *React. Funct. Polym.* **2004**, *59*, 149-154.

[20] C. Xiong, C. Yao, X. Wu, *Hydrometallurgy* **2008**, *90*, 221-226.

[21] Zhu, L.; Xiao, C.; Dai, X.; Li, J.; Gui, D.; Sheng, D.; Chen, L.; Zhou, R.; Chai, Z.; Albrecht-Schmitt, T. E.; Wang, S. *Environ. Sci. Technol. Lett.* **2017**, *4*, 316−322.